Title

Fabrication of uniform vertically-aligned carbon nanotube-polymer composite thin films by capillary flow intrusion

Authors

JinHyeok Cha[1†], Shohei Chiashi[1], Taiki Inoue[1], Erik Einarsson[1‡], Junichiro Shiomi[1], and Shigeo Maruyama[1,2]*

Affiliations

[1]Department of Mechanical Engineering, The University of Tokyo, Bunkyo, Tokyo 113-8656, Japan

[2] Energy NanoEngineering Lab., National Institute of Advanced Industrial Science and Technology (AIST), Tsukuba, 305-8564, Japan

[†] Present address: Materials Development Center, Hyundai Motor Co., Uiwang, Gyeonggi 16082, Republic of Korea

[‡] Present address: Department of Electrical Engineering, The University of Buffalo, Buffalo, NY, 14260, USA

*E-mail: maruyama@photon.t.u-tokyo.ac.jp

Abstract

Polymer and nanomaterial composites, known as nanocomposites, are advanced materials that have many potential applications. One type of thin-film nanocomposite is a polymer-carbon nanotube (CNT) nanocomposite, whose properties are strongly dependent on the uniformity and alignment of CNTs in the nanocomposite. However, the control of CNT alignment in these nanocomposites is still difficult to achieve. Here, we propose a facile single-step method, a capillary flow intrusion method, to fabricate uniform polymer nanocomposite thin films of vertically aligned (VA) single-/multi-walled CNTs that range from 15 to 300 μm in thickness. Raman scattering spectroscopy and polarized Raman spectroscopy measurements, and cross-sectional scanning electron microscopy (SEM) observations confirmed that the polymer was uniformly infiltrated into VACNTs, such that the alignment of CNTs in the nanocomposite was preserved and there were no excess portions of the polymer. Experimental and numerical calculation results indicated that capillary flow rate, wettability, and polymer shrinkage are important factors in the capillary flow intrusion method.

1. Introduction

Aligned carbon nanotubes (CNTs) with exceptional physical properties have garnered attention as fillers in polymer nanocomposites for various applications.[1] Polymer-aligned CNT composites are strongly reinforced in terms of their mechanical properties and they are used as advanced surface materials in aircraft.[2] The high thermal conductivity of CNTs makes polymer-CNT nanocomposites a potential solution for the thermal management of micro-/nanosized electronic devices.[3,4]

Thin films of polymer-aligned CNT nanocomposites are a particularly important material, for which several fabrication methods have been proposed.[2,5] Although these methods provide polymer-CNT nanocomposites, the composites are not uniform and they generally include an excess portion of a polymer that contains few CNTs and thus degrades the physical properties of the nanocomposite. Removal of the excess portions in the case of thin films is difficult; therefore, a fabrication process that do not cause the formation of these excess portions is required.[2]

The orientation of the CNTs in polymer nanocomposites is also crucial with respect to the enhancement of the mechanical[5], thermal[6], and electrical[7] properties. Although the sonication technique is widely used for the dispersion of CNTs in polymers[8,9], it is available only for low concentrations of CNTs in polymers, and it results in the random orientation of the CNTs. In addition, it is difficult to uniformly disperse a high volume fraction of CNTs in a polymer[10] due to the formation of bundle structures.[11]

Although Kimura et al.[12] employed a strong magnetic field to align CNTs dispersed in solution to take advantage of their exceptional anisotropic physical properties, alignment with a magnetic field is also only available for low concentrations of CNTs. Without dispersion treatment, Wardle et al.[10] utilized capillary-induced wetting of

epoxy into vertically aligned CNTs (VACNTs), whose lengths ranged from hundreds of micrometers to a few millimeters. This method also results in a nanocomposite that contains uniform and highly aligned CNT forests in a high volume fraction. However, this method was limited to thick VACNT films, and it is difficult to reduce the film thickness without degradation of the CNT alignment by polishing[2] or the frame for polymer casting.[13] Polydimethylsiloxane (PDMS) is one of the most frequently adopted polymers for the production of nanocomposites with CNTs due to its nontoxicity, flexibility, thermal stability, and biocompatibility. In particular, PDMS is the most attractive candidate polymer for flexible electronic device applications.[5,13–15] PDMS nanocomposites that contain CNTs have been studied to fully utilize the advantages of both CNT and PDMS with respect to the fabrication process[5], enhancement of physical properties [16–18], and the design for micro- and nanofluidic devices.[19]

In this study, a single-step facile method, which is referred to as the *capillary flow intrusion method*, is proposed for the fabrication of uniformly well-infiltrated PDMS-CNT nanocomposites. VA single- and multi-walled carbon nanotubes (SWNTs and MWNTs) films with thicknesses ranging from 15 to 300 μm were fabricated by the capillary flow intrusion method. Raman scattering spectroscopy, polarized Raman spectroscopy and cross-sectional scanning electron microscopy (SEM) observation were then carried out to characterize the infiltration of the polymer, preservation of the CNT orientation, and the uniformity of the nanocomposite. The results reveal that the capillary flow intrusion method enables uniform PDMS infiltration into the entire film maintaining the alignment of CNTs.

2. Methods

Both VASWNTs and VAMWNTs were employed to study the effects of CNT length, diameter, and wall-number on the fabrication of the nanocomposites. VASWNTs were synthesized by alcohol catalytic chemical vapor deposition (ACCVD).[20] Metal catalyst particles were prepared by a dip-coating method using a bimetal catalyst of Co/Mo[21] on a Si substrate. At 800 °C, which is the growth temperature for CNTs, ethanol was introduced to the substrates with catalysts at a flow rate of 450 sccm for 10 min at 1.3 kPa. The lengths of the grown VASWNTs ranged from 15 to 25 μm. VAMWNTs were also synthesized by ACCVD using a Si substrate that was sputtered with 0.5-nm-thick Co and 15-nm-thick Al_2O_3. During the growth of VAMWNTs at 800 °C, ethanol was flowed at a rate of 50 sccm for 15 min. The lengths of the grown VAMWNTs ranged from 40 to 300 μm.

VACNT nanocomposites were fabricated using a liquid-state PDMS premixture (Dow Corning, Sylgard 184). The agent and the base of the PDMS were mixed at a weight ratio of 10:1 and ultrasonicated for 10 min, followed by degassing in a vacuum chamber to remove any trapped air bubbles.

Figure 1 shows the process for the fabrication of the nanocomposites by the capillary flow intrusion method. After mixing a curing agent and the base matrix of PDMS, liquefied PDMS was poured onto an as-grown VACNT forest on a Si substrate using a pipette. As shown in Fig. 1(b), liquefied PDMS does not readily infiltrate into the VACNT forest due to its high viscosity, and a large amount of excess PDMS remains on the top of the CNT forest. Therefore, to remove the excess liquefied PDMS, the substrate was tilted by 90°, as shown in Fig. 1(c). Once complete PDMS coverage on the top of the VACNT forests was achieved, the sample was cured in a vacuum at room

temperature for 48 h to polymerize PDMS. This long curing time was sufficient for the excess PDMS on the top of the aligned CNT forest to flow down into the CNT forest by capillary action.

SEM (Hitachi S-4800, 1 kV acceleration voltage) was carried out to measure the length of the VACNTs, and the thickness of nanocomposite thin films. Transmission electron microscopy (TEM; JOEL JEM-2000EX, 120 kV acceleration voltage) was carried out to investigate the distributions of the wall-number and diameter of CNTs. The detailed structure of the PDMS-VASWNT nanocomposite films was characterized by resonance Raman spectroscopy (Chromex 501is spectrometer with Andor DV401-FI CCD camera) with an excitation laser wavelength of 488 nm and an intensity of 30 μW using a 50× objective lens to achieve a laser spot diameter of ca. 1.5 μm. The intensity change of the G-band and PDMS peaks were compared. To evaluate the alignment of CNTs in the nanocomposite, polarized Raman spectroscopy was performed. The polarization directions of both the excitation laser and the scattered light was set parallel to the vertical alignment direction of the CNTs, and the decrease in the G-band intensity was investigated as a function of polarization angle from 0 to 90° by sample rotation.

3. Results and discussion

3.1 Characterization of PDMS-VACNT composites

Figure 2 shows the Raman scattering spectra from as-grown VASWNTs and VAMWNTs, and their respective PDMS nanocomposites. Both as-grown VASWNTs and the VASWNT-PDMS composite exhibited similarly low D-band to G-band ratios, which verified that no damage to the VASWNTs occurred during the polymerization process. Although a slight change in the radial breathing mode (RBM) peaks was observed, this was attributed to the change in the environment surrounding the VASWNTs. Figures 2(c) and 2(d) show Raman spectra of the VAMWNTs and the PDMS nanocomposite containing VAMWNTs, where almost no difference is evident between them. The fabrication process of the VAMWNT nanocomposite thus also caused no damage to the VAMWNTs. In addition, the wall-number distribution of the VAMWNTs was investigated by TEM (see Fig. 3). The results indicate that the VAMWNTs consist mostly of double-/triple- walled CNTs with diameters ranging from 5 to 20 nm; therefore, although these are referred to as VAMWNTs for simplicity, they do include a few SWNTs.

A comparison of cross-sectional SEM images of the as-grown VASWNTs and the nanocomposite film [see Figs. 4(a) and (b)] reveals that the PDMS completely infiltrated into the VASWNT forest, and the nanocomposite film has the same thickness as the as-grown VASWNTs. Despite the relatively shorter lengths of the VASWNT forests, PDMS was optimally blended with the VASWNT forest.

In addition, in the case of the VAMNTs, the thickness of the PDMS nanocomposite was almost the same as that of the as-grown VAMWNTs, which was approximately 90 to 95 μm [see Figs. 4(c) and (d)]. The capillary flow intrusion method

was successful for the fabrication of nanocomposite films that included VACNT forests with a wide range of thicknesses (from 15 to 300 μm), and the thicknesses of the nanocomposite films were identical to those of the as-grown VACNTs.

The detailed structure of PDMS in the VASWNT composite films was investigated by scanning a cross section of the nanocomposite by Raman spectroscopy. The excitation laser spot for Raman scattering measurements was scanned along the axial direction of the VASWNTs. Figure 5 shows peaks from Si (at 521 cm^{-1}), CNTs (at 1593 cm^{-1}), and PDMS (at 2096 cm^{-1}), where their intensities were dependent on the laser position. Figure 5(b) shows a clear border, where the intensity of the Si peak decreased and both the G-band and PDMS peaks increased. The positional dependence of the G-band was in agreement with that of the PDMS peak intensity, which indicates that the PDMS reached the SWNT-Si interface and no overlayer of PDMS was formed.

In addition to the infiltration of the polymer, the orientation of CNTs in the PDMS matrix plays an important role in enhancing the physical properties of the nanocomposite due to the anisotropic structure of CNTs.[5–7] Thus, the vertical alignment of the CNT forest with preservation of the as-grown morphology in a PDMS matrix can realize optimal performance as a nanocomposite. The alignment of the VASWNTs in the nanocomposite films was thus examined by polarized Raman scattering spectroscopy. Figure 6(a) shows the intensities of the G-band with respect to the angle θ between the VASWNT alignment direction and the polarization of the Raman laser. Figure 6(a) shows that the intensity of the G-band decreases with increasing θ from 0 to 90°.[22] This illustrates the vertical alignment of the as-grown SWNTs used here. Figure 6(b) shows the intensities of the G-band for the VASWNTs that are embedded in the nanocomposite film. The similar variations of intensity as a function of θ for both cases indicate that the

original vertical alignment of the as-grown CNTs was preserved in the PDMS matrix. Both insets show Raman scattering spectra as a function of the polarization angle of the excitation laser.

Because we expected the increase in thermal conductivity, we are planning to measure the thermal conductivity of the nanocomposites by the 3ω method. The 3ω technique is used to provide accurate and reliable measurements of the thermal conductivity of thin films where a thin metal wire is deposited on a nanocomposite to function both as a resistive heater driven with AC current at the frequency ω and as a resistance temperature detector. For better understanding of each fabrication step and the thermal property of the nanocomposite, the results of the measurement of thermal conductivity will be discussed in the future.

3.2 Mechanism of the capillary flow intrusion method

In this section, the mechanism of polymer infiltration into the VACNTs is discussed. To simplify the model, VACNTs are regarded as pillars that stand in a hexagonal network, where the spacing between neighboring pillars is denoted as *r*. Moreover, the infiltration of liquefied polymer is regarded as a flow into a cylindrical tube with the radius *r*. The Washburn equation, also known as the *Lucas-Washburn equation*, describes the capillary flow rate of fluid in a cylindrical tube.[23] By applying Poiseuille's law to fluid motion in a circular tube with a fully wettable capillary, the equation can be written as

$$l = \sqrt{\frac{r\gamma\cos\theta}{2\eta}t}\,, \qquad (1)$$

where *l*, *t*, and η are the penetration distance, time, and dynamic viscosity of the fluid, respectively. *r*, γ, and θ, correspond to the radius of the cylinder, the surface tension, and

the contact angle of the liquid on the capillary, respectively. The capillary flow rate of the fluid, *dl*/*dt*, is given as

$$\frac{dl}{dt} = v = \frac{1}{2}\left(\frac{r\gamma\cos\theta}{2\eta}\right)^{\frac{1}{2}} t^{\frac{1}{2}}. \quad (2)$$

The flow rate of PDMS can be estimated from Eq. (2). r, γ, and η of PDMS are 26 nm [24], 0.0251 N/m[25], and 5 N·s/m^2, respectively. On the other hand, the rate of the flow of liquefied PDMS was measured to be approximately 2.5 mm/s. The rate of PDMS flow was much higher than that of the capillary flow due to high viscosity of PDMS; therefore, once PDMS uniformly covered the top surface of the VACNT forest, capillary flow along the tube axis then occurred.

CNTs are attracted by surface tension, as shown in Fig. 7, and they were balanced, so the structure of the VACNTs did not collapse. The wettability of a fluid is also an important factor for the structural preservation of VASWNTs. The contact angle of PDMS is close to 0° [26], which enables the wetting of nanotubes. Although capillary flow rate and wettability are important in the infiltration process, shrinkage of the polymer also determines the structural preservation of CNTs. PDMS shrinks by less than 1% during the polymerization process.[27] Although polyvinyl alcohol (PVA) has a similar viscosity to PDMS, its volume shrinks significantly during the drying process[28]; therefore, it is difficult to avoid structural changes of the CNTs in PVA composites.

In addition, we have measured thermal conductivity of the nanocomposites to specify the expectation of enhancement to take their anisotropic advantage, and the obtained results will be revealed next publications.

4. Conclusions

We have developed a single-step facile method, referred to as the capillary flow intrusion method, to fabricate uniformly well-infiltrated polymer nanocomposite films of VACNTs with thicknesses ranging from 15 to 300 μm without the formation of excess polymer portions. Raman scattering spectroscopy, polarized Raman spectroscopy, and cross-sectional SEM observation were carried out to characterize the infiltration of the polymer, the preservation of the CNT orientation, and the uniformity of the nanocomposite. On basis of the results, it was confirmed that PDMS uniformly infiltrates into the VACNT film by capillarity without deterioration of the aligned morphology. The mechanism was clarified with consideration of three factors: capillary flow rate, wettability, and polymer shrinkage.

Acknowledgment

Part of this work was financially supported by JSPS KAKENHI Grant Number JP15H05760.

5. Reference

1) M. S. Dresselhaus, G. Dresselhaus, and P. C. Eklund, *Science of Fullerenes and Carbon Nanotubes* (Academic Press, New York, 1996).

2) H. Cebeci, R. G. De Villoria, A. J. Hart, and B. L. Wardle, Compos. Sci. Technol. **69**, 2649 (2009).

3) M. J. Biercuk, M. C. Llaguno, M. Radosavljevic, J. K. Hyun, A. T. Johnson, and J. E. Fischer, Appl. Phys. Lett. **80**, 2767 (2002).

4) R. Mahajan, Intel Technol. J. **06**, 62 (2002).

5) A. T. Sepúlveda, R. Guzman de Villoria, J. C. Viana, A. J. Pontes, B. L. Wardle, and L. A Rocha, Nanoscale **5**, 4847 (2013).

6) H. Huang, C. H. Liu, Y. Wu, and S. Fan, Adv. Mater. **17**, 1652 (2005).

7) H. Peng and X. Sun, Chem. Phys. Lett. **471**, 103 (2009).

8) A. Allaoui, S. Hoa, and M. Pugh, Compos. Sci. Technol. **68**, 410 (2008).

9) S. Harish, K. Ishikawa, E. Einarsson, S. Aikawa, S. Chiashi, J. Shiomi, and S. Maruyama, Int. J. Heat Mass Transf. **55**, 3885 (2012).

10) B. L. Wardle, D. S. Saito, E. J. García, A. J. Hart, R. G. de Villoria, and E. A. Verploegen, Adv. Mater. **20**, 2707 (2008).

11) K. Bui, B. P. Grady, and D. V. Papavassiliou, Chem. Phys. Lett. **508**, 248 (2011).

12) T. Kimura, H. Ago, M. Tobita, S. Ohshima, M. Kyotani, and M. Yumura, Adv. Mater. **14**, 1380 (2002).

13) A. T. Sepúlveda, R. G. De Villoria, J. C. Viana, A. J. Pontes, B. L. Wardle, and L. A. Rocha, Procedia Eng. **47**, 1177 (2012).

14) D. Kim, J. Han, H. Park, and K. Yun, Solid-State Sensors, Actuators Microsystems Conf., 2011, p.2355.

15) L. Chen, C. Liu, K. Liu, C. Meng, C. Hu, and J. Wang, ACS Nano **5**, 1588 (2011).

16) J. Salzbrenner, C. Apblett, and T. Khraishi, Polym. Int. **62**, 608 (2013).

17) J. Hong, J. Lee, C. K. Hong, and S. E. Shim, Curr. Appl. Phys. **10**, 359 (2010).

18) A. Khosla and B. L. Gray, Mater. Lett. **63**, 1203 (2009).

19) J. Oh, G. Kim, D. Mattia, and H. (Moses) Noh, Sens. Actuators, B **154**, 67 (2011).

20) Y. Murakami, Chem. Phys. Lett. **385**, 298 (2004).

21) Y. Murakami, Y. Miyauchi, S. Chiashi, and S. Maruyama, Chem. Phys. Lett. **377**, 49 (2003).

22) Z. Zhang, E. Einarsson, Y. Murakami, Y. Miyauchi, and S. Maruyama, Phys. Rev. B **81**,165442 (2010).

23) E. W. Washburn, Phys. Rev. **17**, 273 (1921).

24) E. Einarsson, H. Shiozawa, C. Kramberger, M. H. Rummeli, A. Gruneis, P. Thomas, and S. Maruyama, J. Phys. Chem. C **111**, 17861 (2007).

25) J. Mark, *Polymer Data Handbook* (Oxford University Press, New York, 1999).

26) A. Barber, S. Cohen, and H. Wagner, Phys. Rev. Lett. **92**, 186103 (2004).

27) Y. Xia and G. Whitesides, Annu. Rev. Mater. Sci. **28**, 153 (1998).

28) C. P. Derdeyn, C. J. Moran, D. T. Cross, H. H. Dietrich, and R. G. Dacey, Am. J. Neuroradiol. **16**, 1335 (1995).

Caption

Figure 1 (Color online)

Fabrication process of CNT-PDMS nanocomposite by the capillary flow intrusion method. (a) VASWNTs and VAMWNTs are grown on Si substrate, and (b) PDMS is poured onto the CNT forests with a pipette. (c) By tilting the substrate up to 90°, PDMS infiltrated naturally into the VACNTs forests by capillarity. Excess PDMS flows down over aligned CNT forest. (d) Through the polymerization (curing) for 48 hours at room temperature, the composite has the same thickness as the lengths of aligned CNTs.

Figure 2 (Color online)

Raman scattering spectra of the RBM (left) and D-/G-band (right) range of (a) as-grown VASWNTs, (b) VASWNTs in PDMS nanocomposite, (c) as-grown VAMWNTs, and (d) VAMWNTs in PDMS nanocomposite.

Figure 3

(a) TEM image of MWNTs. (b) Wall number distribution of CNTs, which indicates that the VAMWNTs consist mostly of double-/triple-walled CNTs

Figure 4

(a) Cross-sectional SEM images of 20-22-μm-long as-grown VASWNT forest and (b) PDMS nanocomposite with the VASWNT forest fabricated by the capillary flow intrusion method. This shows that the thickness of the nanocomposite is the same as the

length of the as-grown VASWNT forest without an over-layer of PDMS. (c) Cross-sectional SEM images of 90-95 μm long as-grown VAMWNT forest, and (d) corresponding PDMS nanocomposite.

Figure 5 (Color online)

(a) Raman scattering spectra of Si, G-band of SWNTs and PDMS, and (b) spatial intensity distribution of Raman scatterings along the vertical direction of the nanocomposite. The presence of both G-band of SWNTs and PDMS peak at the same point indicates the complete infiltration of PDMS along the full thickness of the film. The inset SEM image shows the origin of the scan.

Figure 6 (Color online)

Polarized Raman spectra of (a) as-grown VASWNTs and (b) VASWNTs in a PDMS matrix. The original vertical alignment of the as-grown CNTs was preserved in the PDMS matrix, as indicated by comparison of the G-band intensities of VASWNTs. Both insets shows Raman scattering spectra as a function of the polarization angle (θ) of the excitation laser.

Figure 7 (Color online)

Proposed mechanism of PDMS infiltration into CNTs. Capillary flow of PDMS occurs together with a balanced force that acts on each nanotube and leads to a stable structure without collapse due to the high viscosity of PDMS.

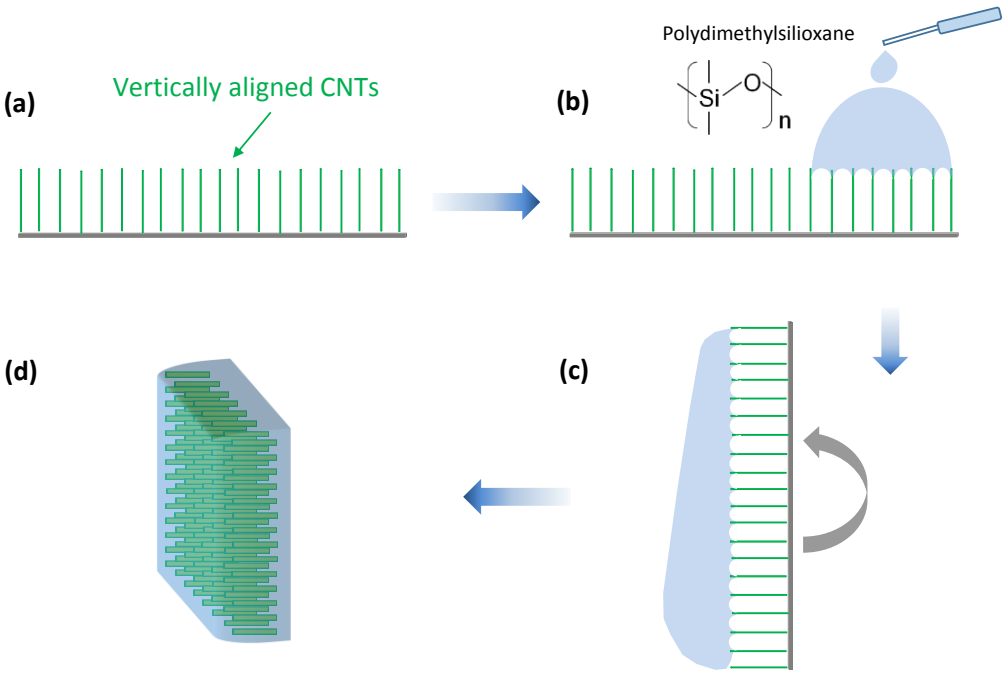
(a)
Vertically aligned CNTs
(b)
Polydimethylsilioxane
Si
O
n
(c)
(d)

Figure 1

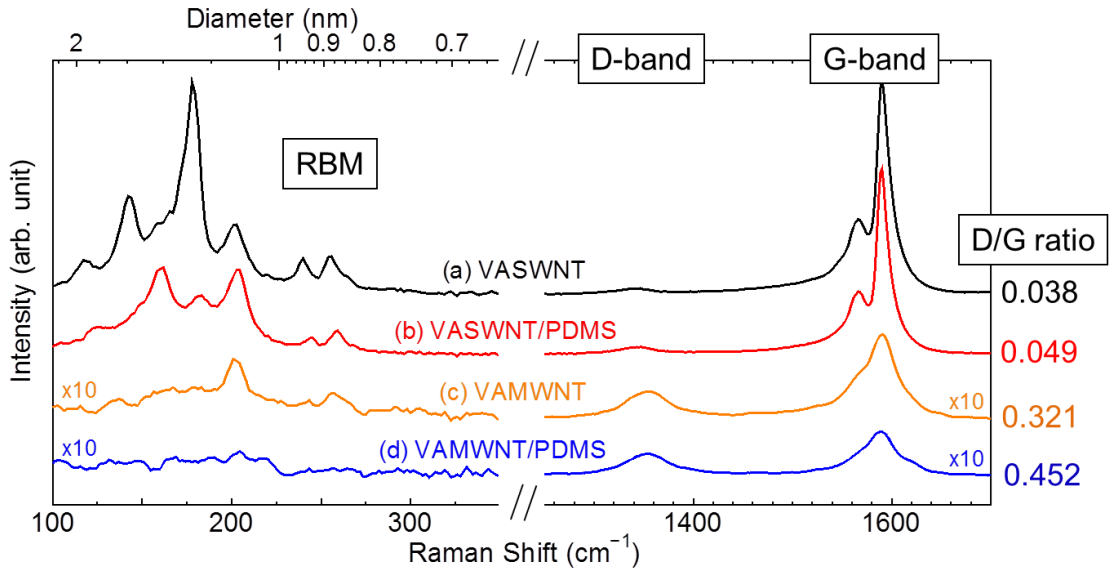
Diameter (nm)
2
1
0.9
0.8
0.7
D-band
G-band
RBM
D/G ratio
(a) VASWNT
0.038
(b) VASWNT/PDMS
0.049
x10
(c) VAMWNT
x10
0.321
x10
(d) VAMWNT/PDMS
x10
0.452
Intensity (arb. unit)
100
200
300
1400
1600
Raman Shift (cm^{-1})

Figure 2

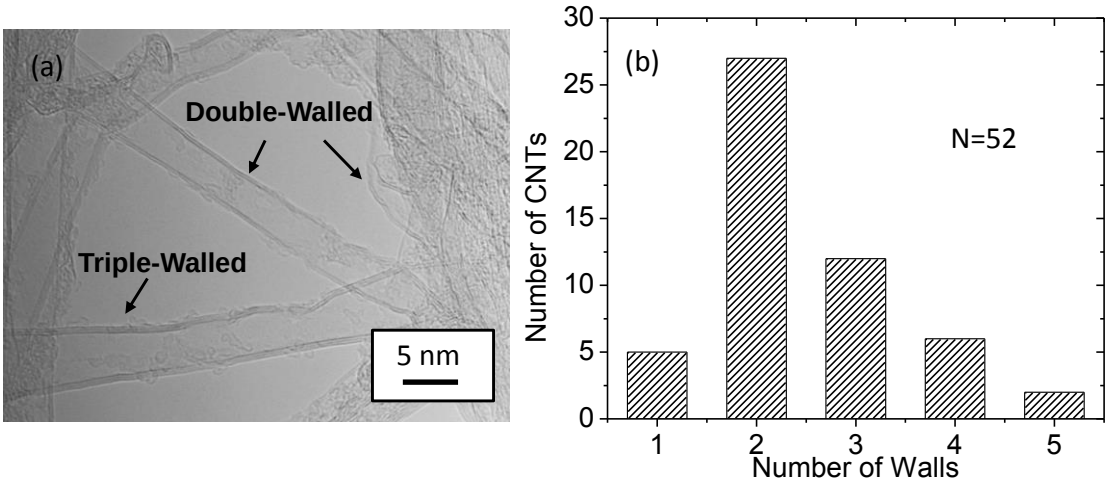
(a)
Double-Walled
Triple-Walled
5 nm
(b)
N=52
Number of CNTs
Number of Walls
0
5
10
15
20
25
30
1
2
3
4
5

Figure 3

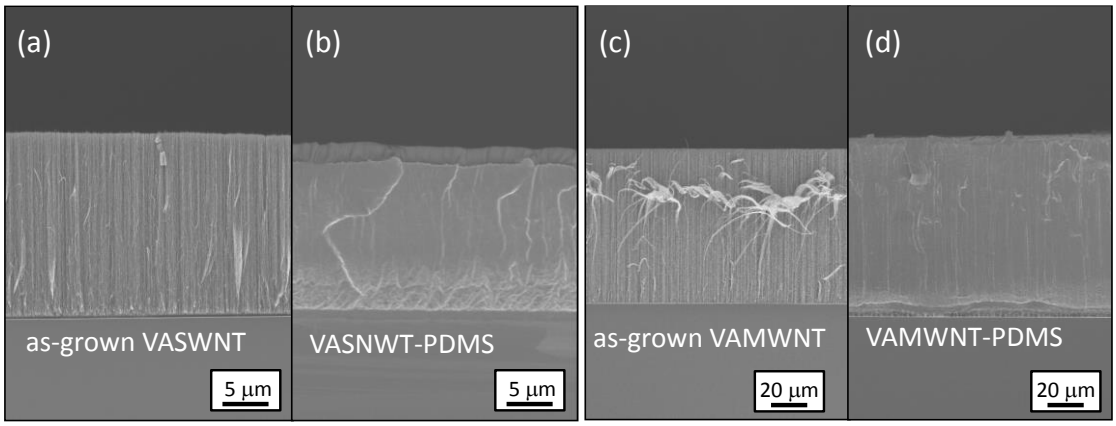
(a)
(b)
(c)
(d)
as-grown VASWNT
5 μm
VASNWT-PDMS
5 μm
as-grown VAMWNT
20 μm
VAMWNT-PDMS
20 μm

Figure 4

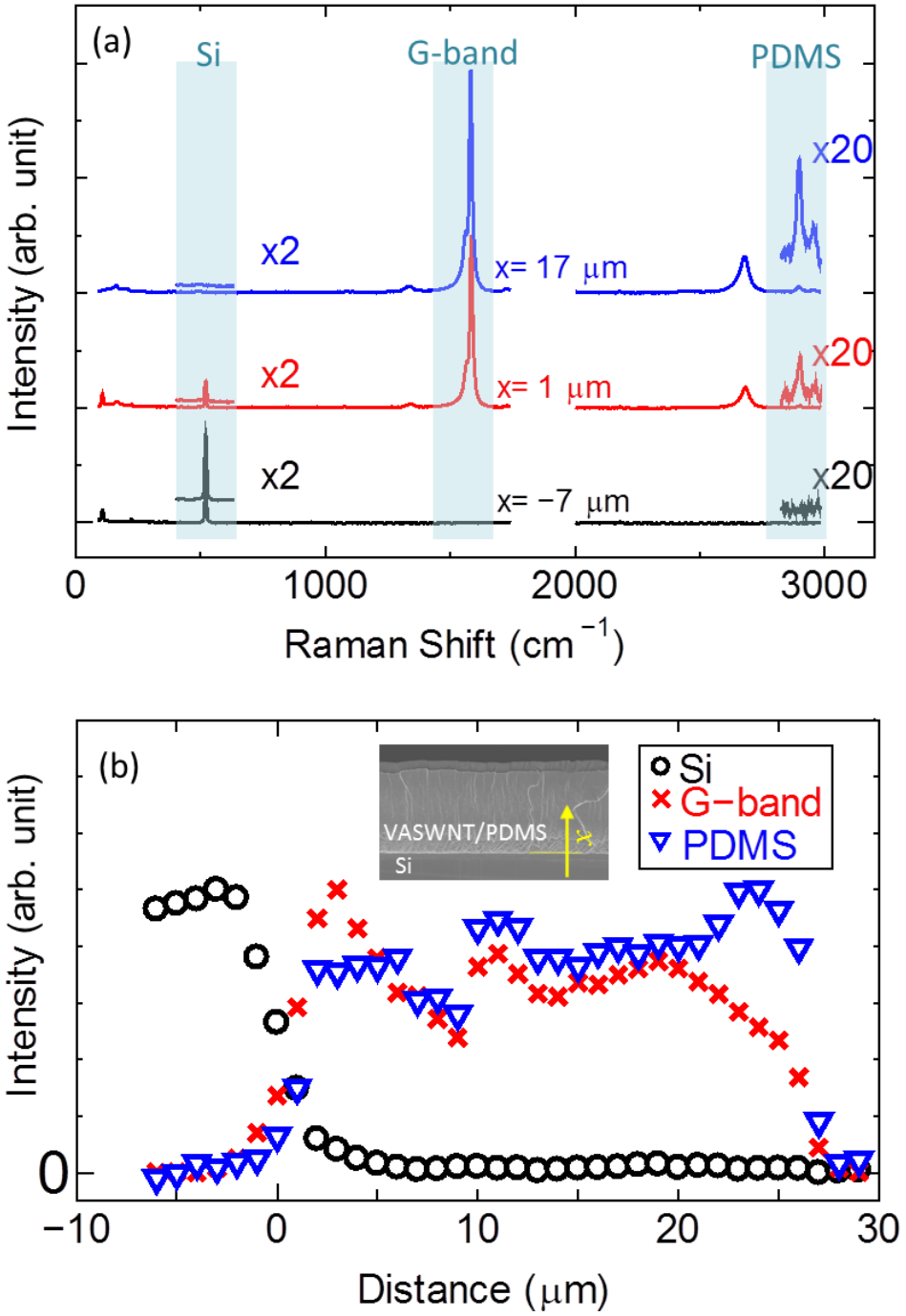
(a)
Si
G-band
PDMS
x20
x2
x= 17 μm
x2
x20
x= 1 μm
x2
x20
x= −7 μm
Intensity (arb. unit)
0
1000
2000
3000
Raman Shift (cm −1)
(b)
VASWNT/PDMS
Si
Si
G−band
PDMS
Intensity (arb. unit)
0
−10
0
10
20
30
Distance (μm)

Figure 5

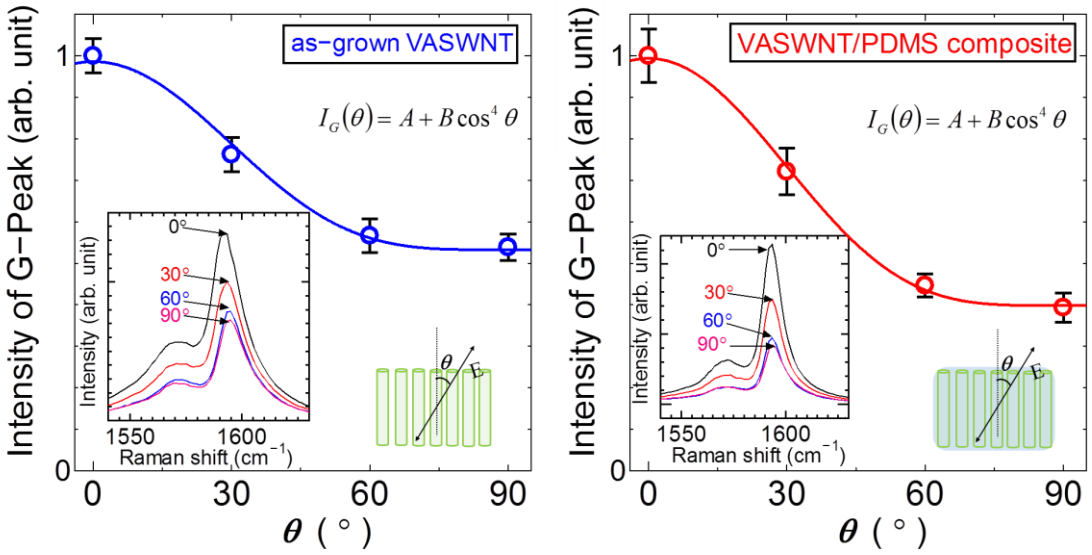
as-grown VASWNT
$I_G(\theta) = A + B\cos^4\theta$
Intensity of G-Peak (arb. unit)
Intensity (arb. unit)
0°
30°
60°
90°
1550
1600
Raman shift (cm^{-1})
θ
E
0
30
60
90
θ (°)
VASWNT/PDMS composite
$I_G(\theta) = A + B\cos^4\theta$
Intensity of G-Peak (arb. unit)
Intensity (arb. unit)
0°
30°
60°
90°
1550
1600
Raman shift (cm^{-1})
θ
E
0
30
60
90
θ (°)

Figure 6

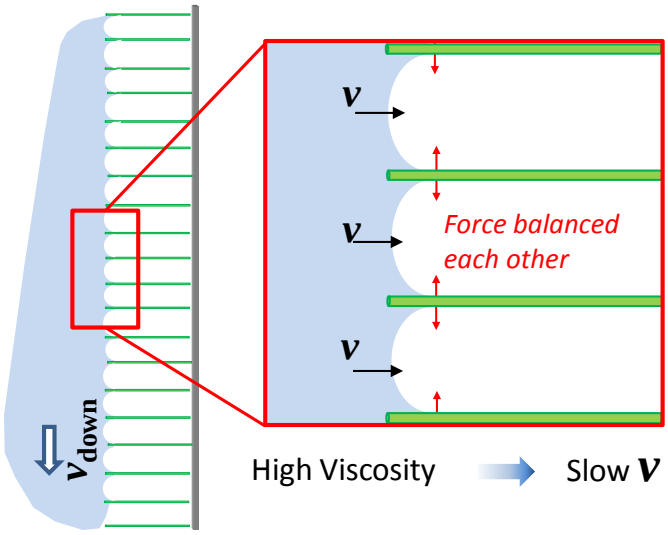

Figure 7